

## Additive Manufacturing of Copolyamide-Modified Magnetic Composites for High-Temperature Bonded Magnets

Pratik U. Karkhanis<sup>1</sup>, Oluwasola K. Arigbabowo<sup>2</sup>, Everest Sweet<sup>1</sup>, Andrew Luis Geise<sup>2</sup>,  
Oleksandr Syzov<sup>2</sup>, Lorenzo Williams<sup>2</sup>, Jitendra S. Tate<sup>1,2</sup>

Ingram School of Engineering<sup>1</sup>  
Materials Science, Engineering, and Commercialization Program<sup>2</sup>  
Texas State University

This research was in-part funded by the National Science Foundation (NSF) under the DMR-MRI program, award number 2216440, and additionally supported by Texas State University's research Thesis Support fellowship.

### Abstract

Additive manufacturing of polymer-bonded magnets has the potential to revolutionize magnet production by enabling more sustainable and customizable fabrication methods. This study focuses on 3D printing a Polyamide-4,6 (PA 4,6) matrix filled with Strontium Ferrite ( $\text{SrFe}_{12}\text{O}_{19}$ ) particles, with an emphasis on improving melt flow during extrusion through the addition of compatible plasticizers and functional additives. To overcome the poor flowability caused by the high crystallinity of PA 4,6, Platamid®, a thermoplastic copolyimide hot-melt adhesive, was introduced as a processing aid. Optimized extrusion and drying methods were also implemented to enhance printability further. Experimental results showed that incorporating Platamid® significantly reduced nozzle clogging and improved first-layer quality during FFF. The composite was fabricated using a twin-screw extruder, and the resulting monofilament and 3D-printed parts were evaluated for mechanical, thermal, and morphological properties. While the addition of Platamid® improved processability, it led to a reduction in mechanical performance, highlighting a trade-off between printability and structural integrity in the additive manufacturing of high-temperature polymer-bonded magnets.

Keywords: Magnetic composite, strontium ferrite powder, twin-screw extruder, PA 4,6, fused filament fabrication, bonded magnets.

## 1. INTRODUCTION

### 1.1 Motivation of Study

Bonded magnetic composites (BMCs) are a promising alternative to traditional sintered magnets. They consist of polymeric binders and magnetic particles and are suitable for the Fused Filament Fabrication (FFF) additive manufacturing process. Compared to conventional sintered magnets, BMCs offer a good combination of mechanical, thermal, and magnetic properties. High-temperature thermoplastics, such as nylons, are a viable choice for high-performance applications in engineering, medical, and research industries.

The chosen material system consists of a polymer binder and a magnetic filler, primarily Polyamide (Nylon) 4.6, and a hard magnetic filler, Strontium Ferrite ( $\text{SrFe}_{12}\text{O}_{19}$ ), which is an engineering thermoplastic that possesses high heat, abrasion, and chemical resistance, as well as toughness, and also demonstrated printability for magnetic composite [11]. This makes it suitable for demanding applications such as automotive, electrical, aerospace, and others. Strontium Ferrite ( $\text{SrFe}_{12}\text{O}_{19}$ ) is a magnetic material used widely in industrial settings, most notably in producing permanent magnets. It possesses desirable magnetic properties such as high saturation and coercivity, which ensure long-term stability. Other benefits include large crystalline anisotropy, corrosion resistance, and affordability compared to rare-earth alternatives.

Combining strontium ferrite with PA 4.6 produces a composite material with strong magnetic performance and structural integrity. However, fabricating PA 4.6- $\text{SrFe}_{12}\text{O}_{19}$  composites presents challenges due to the low melt flow index (MFI) and high crystallinity of Nylon 4.6. These properties can lead to issues such as under-extrusion and nozzle clogging, which result from rapid cooling and shear thickening. This study aims to explore the addition of functional additives, primarily Platamid®, which contains long-chain aliphatic diamines and Dicarboxylic acids that act as plasticizing agents to improve flow and address these challenges.

## 1.2 Literature Review

Huber et al. (2016) investigated the feasibility of using fused deposition modeling (FDM) 3D printing to create polymer-bonded rare-earth magnets as an alternative to traditional injection molding. Their research demonstrated that 3D-printed isotropic NdFeB permanent magnets exhibit comparable magnetic properties to those of molded samples, while allowing for more complex geometries. Printing parameters were optimized using a commercially available printer. Although the printed magnets had slightly lower volumetric mass density and remanence, they still exhibited functional magnetic performance. The study emphasized the potential for customized magnetic systems with tailored field distributions and suggested that further optimization of printing and material parameters could improve performance.[5] Palmero et al. (2019) investigated extrusion-based fabrication of magnetic-polymer composite filaments, focusing on strontium ferrite and NdFeB fillers. Composite pellets with high magnetic powder loadings were embedded in an ethylene ethyl acrylate (EEA) matrix. The extrusion process produced continuous filaments, as confirmed by SEM, which showed well-dispersed magnetic particles. VSM analysis showed that most magnetic properties were preserved in strontium ferrite-based materials, though NdFeB composites experienced slight magnetization loss due to retention in the extruder. A notable achievement was the fabrication of pre-magnetized strips using an applied field, demonstrating the potential of magnetic alignment during 3D printing to enhance anisotropy. [6]

Zhang et al. (2023) presented a comprehensive review of 3D printing techniques for functional magnetic materials, covering methods such as FDM, direct ink writing (DIW), stereolithography (SLA), and powder bed fusion (PBF). They emphasized the advantage of producing complex geometries with tailored magnetic properties, with a key focus on field-assisted printing techniques that align particles in situ to enhance anisotropy. The review also explored emerging applications in soft robotics, electronics, and magneto-thermal devices. Challenges identified included difficulty achieving high particle loading while maintaining printability. Future directions call for improved formulations, higher-resolution techniques, and hybrid processing approaches. [8]

Boparai et al. (2016) developed a Nylon6-Al-Al<sub>2</sub>O<sub>3</sub> composite filament using single-screw extrusion (SSE) for FDM applications. The study systematically varies material composition,

temperature, and mixing parameters. ASTM methods and DMA characterized rheological, mechanical, and thermal properties. The results demonstrated the viability of optimized PA6-based composites for high-performance additive manufacturing. [1]

Xiao et al. (2000) incorporated liquid crystal polymer (LCP) into a polyphenylene sulfide (PPS) matrix containing NdFeB particles to improve melt flow and high-temperature strength. LCP enhanced interfacial adhesion and reduced shear-induced clogging, with its low viscosity supporting consistent extrusion. Adding up to 20 vol% LCP decreased viscosity by approximately 29%, improved stiffness, and increased dimensional stability without compromising magnetic properties. However, the excessive LCP reduced mechanical performance. [7]

Chapman et al. (2020) addressed the poor melt flow of highly crystalline nylon by incorporating various impact modifiers (IM) and chain extenders (CE). With 15% and 20% IM and 0.5 phr CE, crystallinity was reduced by 6.8% and 14.9%, respectively. Enthalpy of crystallization ( $\Delta H_c$ ) dropped from 64.3 J/g to 50.7 J/g, lowering the energy required for phase transition and improving extrusion behavior. [2]

Through an extensive analysis of prior studies, the authors discuss how different AM processing parameters influence key material characteristics, including grain size, phase distribution, and porosity. They reference research that employs characterization techniques such as scanning electron microscopy (SEM) and X-ray diffraction (XRD) to assess structural integrity. At the same time, magnetic performance is evaluated through vibrating sample magnetometry (VSM) and B-H curve analysis. The literature suggests that AM enables the tuning of magnetic properties by adjusting fabrication parameters, offering significant potential for designing application-specific magnetic materials.

Despite the advantages of additive manufacturing (AM) for magnetic materials, the review highlights several challenges that need to be addressed. Common issues include residual stress, oxidation, and the formation of defects, all of which can negatively impact both the structural and functional properties of the materials. The authors discuss various post-processing treatments, such as heat treatment and hot isostatic pressing, which have been explored to mitigate these challenges and enhance material performance. Overall, this review provides a critical analysis of the current state of AM for magnetic materials, identifying both opportunities and limitations. The authors recommend that future research should focus on optimizing processing conditions, improving the quality of material feedstock, and integrating computational modeling to enhance the predictability

and reproducibility of AM-fabricated magnetic components. Their work lays the groundwork for further exploration into the development of advanced magnetic materials through additive manufacturing.

### **1.3 Objectives**

The primary goal of this research is to investigate the feasibility of using various functional additives as plasticizing agents to produce functional 3D printed bonded magnets better. This study focuses on adding additives, Platamid, and optimizing properties to produce an extruded filament suitable for 3D printing on standard FDM printers. Additionally, this research aims to address the issues related to the low MFI and high shear thickening properties of PA 4.6 composite materials and to characterize the physical, mechanical, and chemical properties of the material system. Ultimately, it examines the potential applications of 3D-printed magnets in various industries, including electronics, robotics, medical devices, and energy systems, demonstrating their viability for practical and functional use. In this study, we fabricated a bonded magnetic composite with functional additives and characterized it for its thermal and mechanical behavior. The morphology of the fabricated composite and the printed magnetic filament was explored.

## **2. MATERIALS AND METHODS**

### **2.1 Materials System**

Polyamide-4,6 (PA-4,6) resin is a high-performance polyamide with a melting temperature of approximately 295 °C and a 1.18 g/cm<sup>3</sup> density. It was used as the polymer matrix for the bonded magnetic composites (BMC). Strontium ferrite (SrFe<sub>12</sub>O<sub>19</sub>), a magnetic ceramic powder, was used as the reinforcement filler in the BMC.

Platamid® pellets supplied by Polymer Dynamix are utilized as a flow enhancer to improve the BMC's 3D printing characteristics. Platamid® is a plasticizer-free thermoplastic copolyimide hot melt adhesive (HMA) designed for durable, versatile, and solvent-free bonding across a wide range of substrates, including textiles, plastics, metals, and foams, and used to enhance polymer flow.

## 2.2 Composite materials preparation

To turn both PA-4,6 and Platamid into powder, pellets were added to a high-RPM polymer blender with dry ice. Dry ice is used to maintain cold temperatures, prevent melting due to friction, and enable the pellets to undergo a shearing action. The pellets were added to the blender, and dry ice was added in a 1:1 ratio to the pellets. This was then blended until the dry ice was completely sublimated. Once done, the powder was removed and sifted through a strainer into a collection bin.

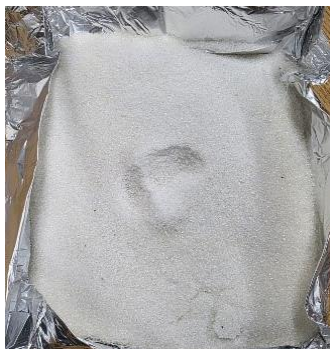


**Figure 1.** Processed Platamid®

The resulting powders were placed in an oven to remove moisture condensed from the sublimation of dry ice. To prevent thermal degradation or melting of the materials, the oven temperature was maintained below the melting points of both polymers, at approximately 100°C, which was sufficient to evaporate residual water. The powders were left in the oven for at least 24 hours to ensure complete drying. The dried powders were manually mixed in a beaker to achieve a uniform dispersion of Platamid® within the PA-4,6 matrix (Figure 2). The beaker was tared on a digital scale, and the powders were weighed to obtain a final blend with a target composition of 90 wt.% of PA-4,6+ 10 wt.% Platamid. To make a matrix blend that is added with filler.



**Figure 2** Hand Mixing of powdered plasticizer with PA 4,6 powder

Strontium Ferrite is used as a magnetic filler. Such powders are typically characterized by their ability to impart magnetic properties when compounded with a polymer matrix. Key features of these magnetic powders include their coercivity, remanence, and magnetic saturation, which define their ability to become magnetized and retain magnetization. The particle size, shape, and distribution within the polymer matrix are crucial for achieving desired magnetic properties and ensuring uniformity in the final composite material. Dowa Electronics Materials Co. provides the Strontium Ferrite particles used in this extrusion. The magnetic particles play a role in the magnetic characteristics of both the composite filament and the characterization samples produced using the FDM technique. The parameters of the magnetic strontium ferrite particles used in this thesis project are presented in Table 1.

**Table 1:-** Key physical, thermal, and magnetic properties of Strontium Ferrite ( $\text{SrFe}_{12}\text{O}_{19}$ ).

Property	Specification	Description
<b>Chemical Formula</b>	$\text{SrFe}_{12}\text{O}_{19}$	Strontium Ferrite belongs to the ferrite class of magnetic oxides.
<b>Magnetic Property</b>	Ferrimagnetic	Exhibits ferrimagnetism, a type of permanent magnetism.
<b>Curie Temperature</b>	$\sim 450^\circ\text{C}$	The temperature above which the material loses its permanent magnetic properties.
<b>Density</b>	$\sim 5 \text{ g/cm}^3$	Indicates the mass per unit volume, relevant for weight considerations in applications.
<b>Particle Size</b>	Varies (Nano to Micrometer range)	The size of the particles, which can affect the magnetic properties and the dispersion in composites.
<b>Thermal Stability</b>	Good	Maintains magnetic properties over a range of temperatures.
<b>Corrosion Resistance</b>	Moderate	Resistance to corrosion, important for longevity in certain applications.
<b>Electrical Resistivity</b>	High	Exhibits high electrical resistivity, beneficial for certain applications.

### 2.3 Filament Fabrication via Twin Screw Extrusion

A Thermo Scientific Process 11 co-rotating twin-screw extruder (Figure 3) was used to fabricate the composite filaments, providing precise control over material mixing and feeding. Prior to extrusion, a series of calibration runs were conducted to ensure that the feed rates of PA-4,6 powder and strontium ferrite ( $\text{SrFe}_{12}\text{O}_{19}$ ) particles matched the targeted weight ratios in the

final composites. Experimental trials were performed using blends of PA 4,6 and Platamid with strontium ferrite at weight ratios ranging from 90:10 to 70:30.

The PA-4,6 powder was loaded into a volumetric screw feeder (Feeder 1), and different RPM settings were tested in one-minute intervals. With the extruder barrel left open, the transported powder was collected in a beaker and weighed. This procedure was repeated until the feed rate reached the desired throughput of 10 g/min, which is the optimal input rate for the Process 11 extruder. For reference, this corresponds to approximately 9 g/min for a 90:10 mix and 7 g/min for a 70:30 mix. Calibration was essential to ensure stable extrusion and to prevent issues such as clogging or void formation. A similar calibration procedure was carried out for the strontium ferrite particles using volumetric screw feeder 2. This feeder was adjusted through one-minute trials until the collected ferrite mass matched the intended weight percentage for each formulation. This approach ensured accurate proportioning of both the polymer and the magnetic filler during extrusion, enabling the production of uniform composite filaments.

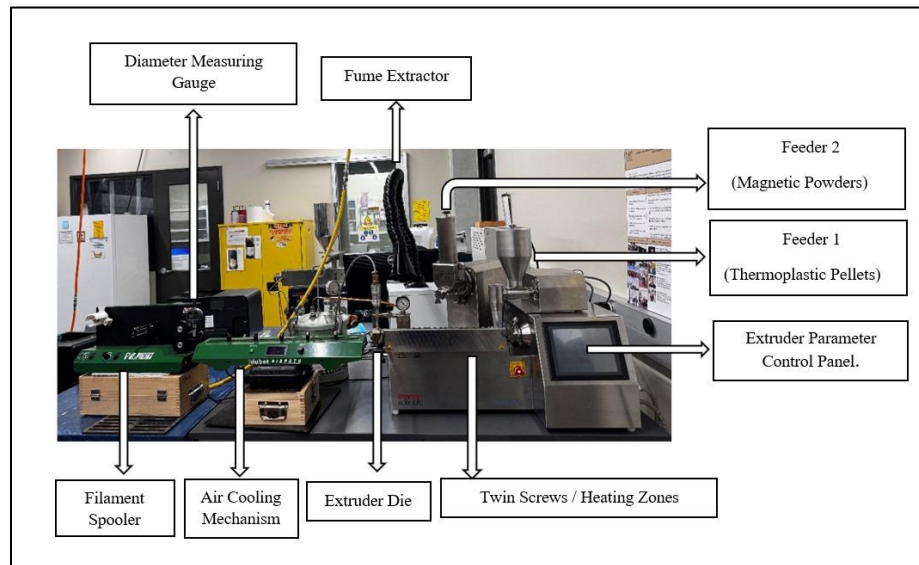


**Figure 3. Twin screw extruder setup**

After calculating the feed rates and performing the initial calibration as discussed above, the first extrusion cycle was conducted to achieve a consistent filament diameter. The nominal value of  $1.75 \pm 0.05$  mm was targeted, a standard in modern 3D printers [9], including the one used in the lab. The twin-screw extruder used was the Thermo Scientific Process 11 Parallel Twin-Screw Extruder, featuring a corotating arrangement with 11 mm diameter screws and a length-to-

diameter ratio of 40:1. Process 11 is equipped with three multifunctional barrel ports for feeding and venting purposes, as well as eight heating zones to control the extrusion temperature process.

Since the first cycle was experimental, only the PA-4,6 powder was extruded to avoid the unwanted loss of strontium ferrite particles. To ensure accuracy, the diameter was measured constantly using a caliper in two directions each time. During extrusion, the adjustments were made to the drive speed of the filament winder and the airflow speed in the airpath until a combination was achieved that produced the desired diameter. The out-of-specification filament was cut and discarded.

The final round of extrusion was performed using the adjusted parameters (Figure 4 & Figure 5):

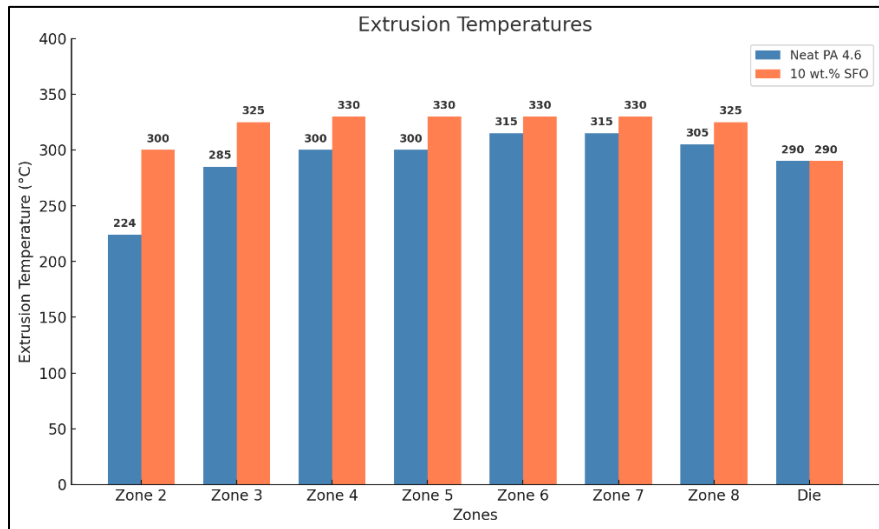


Figure 4. Extrusion Temperatures

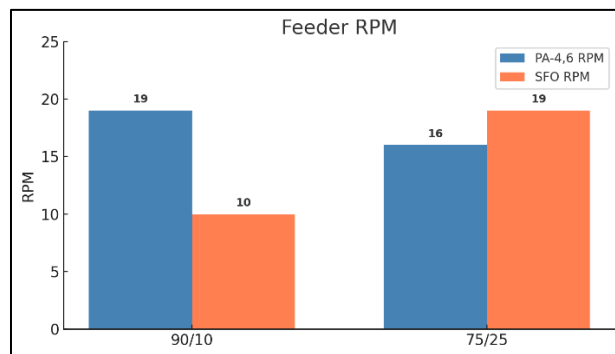


Figure 5. RPM of Feeder 1 and Feeder 2

Both screw feeders were connected to the twin-screw extruder. A standard die with a conical insert and an orifice diameter of 1.75 mm was used to shape the filament. Having left the die, the filament underwent forced convection cooling. The cooling unit used was Airpath by Fila Bot, Figure 6, having the following specifications:

Table 2. Airpath Specifications

<b>Power Requirements</b>	110/220 VAC, 50/60 Hz
<b>Noise Level</b>	About 50dB at max speed
<b>Dimensions (L × W × H)</b>	24 × 7.25 × 3.5 in (60.96 × 18.42 × 8.89 cm)
<b>Weight (mass)</b>	9 lbs (4.08 kg)



Figure 6. Airpath by Filabot

Air cooling was selected for filament production due to the need for rapid cooling, which is essential for maintaining uniform dimensional stability [3]. Slow cooling of highly crystalline PA-4,6 can result in uneven shrinkage, internal stress development, and dimensional distortion. Additionally, given the hygroscopic nature of PA-4,6, which readily absorbs moisture, water-based cooling methods could adversely affect its mechanical integrity and dimensional consistency. The filament was manually spooled while the FilaBot Spooler precisely guided it. The resulting spools with filament were stored in an oven at 80 °C for a minimum of 24 hours to minimize the impact of moisture during the final printing steps.

## 2.4 FDM-Based 3D Printing

Incorporating hot melt adhesive into the composite filament formulation significantly influenced the flow characteristics during the 3D printing process. Compared to unmodified composite filaments, the hot-melt adhesive-modified filaments exhibited improved flow consistency. To keep up with the melt flow printing speed, the printing speed was increased from 5 mm/s to 10 mm/s to optimize print quality. This adjustment contributed to a smoother surface finish and enhanced layer uniformity in the final printed magnetic composite parts. The printing process remained stable and

uninterrupted despite the modified flow behavior no nozzle clogging or extrusion issues were encountered throughout the operation. These results demonstrate the effectiveness of hot-melt adhesive in enabling reliable high-speed printing of magnetic composite filaments. As shown in Figure 8, an improvement in surface quality and uniform print can be observed, which is a result of the addition of Platamid in the material system.

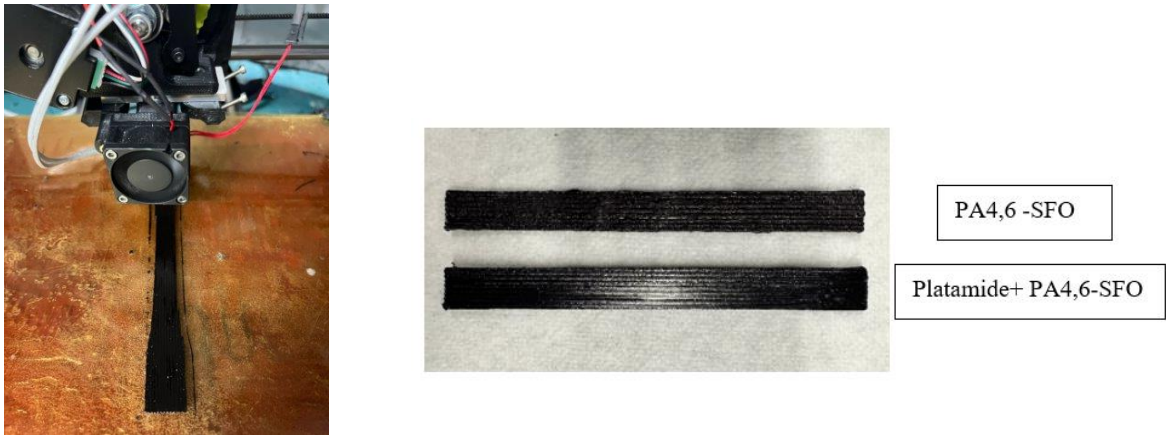


**Figure 7.** Printing of Bonded Magnetic composite    **Figure 8 :-** PA4,6- 10wt% SFO and to 10wt% SFO Platamid composite

The extruded and dried filament was used in 3D printing bonded magnets with a rectangular cross-section using the LulzBot TAZ4 3D printer with parameters listed in table 3.

**Table 3.** Printing parameters

<b>Printing temperature</b>	340 C
<b>Bed temperature</b>	135 C
<b>Printing speed</b>	10 mm/s
<b>Infill density</b>	100%
<b>Layer height</b>	0.2 mm

### 3. MATERIALS CHARACTERIZATION.

#### 3.1. Scanning Electron Microscopy

The morphology was analyzed using JEOL scanning electron microscopy (JEOL SEM). A scanning electron microscope (SEM) was used to examine the composition of the magnetic fillers in strontium ferrites and validate the dispersion of the bonded magnetic composites at the JOEL SEM facility at Texas State University. The results showed good dispersion of the strontium ferrite into the PA 4.6 matrix.

Setup of each Image taken is illustrated in table 4, FP stands for filament with plasticizer, F/P stands for filament without plasticizer. The .1 and .2 following refer to minimal zoom (.1) and maximum zoom (.2) for the respective sample.

**Table 4.** SEM image settings

Parameter	FP.1	FP.2	F/P.1	F/P.2	PP.1	PP.2	P/P.1	P/P.2
Type	SEI	SEI	BEC	BEC	SEI	SEI	BEC	BEC
Magn.	X1000	X5000	X1000	X5000	X1000	X4300	X1200	X4300
Res.	10 $\mu\text{m}$	5 $\mu\text{m}$	10 $\mu\text{m}$	5 $\mu\text{m}$	10 $\mu\text{m}$	5 $\mu\text{m}$	10 $\mu\text{m}$	5 $\mu\text{m}$
Voltage	20 kV	20 kV	20 kV	20 kV	15 kV	15 kV	20 kV	20 kV
Spot Size	50	50	60	60	50	50	55	55

Starting with the extruded filament, we have two main types. One sample had no plasticizer and a combination of 10 wt% strontium ferrite in the PA-4,6 matrix Figure 9 and Figure 10 , while the other sample had a plasticizer in the filament, Platamid, at 15 wt%. As shown in Figure 12, there is good dispersion. Following this, the filament containing the plasticizer was extruded.

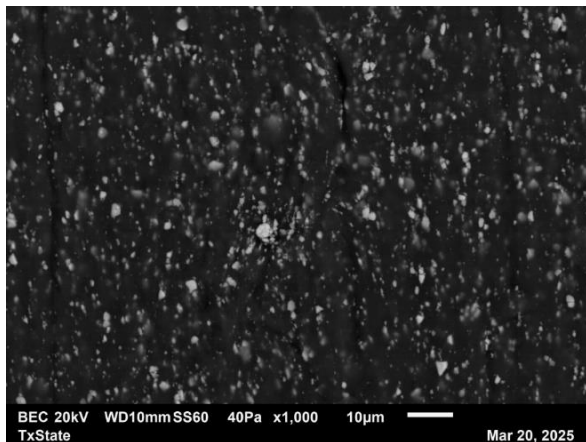


**Figure 9.** Filament with no plasticizer, 1000X

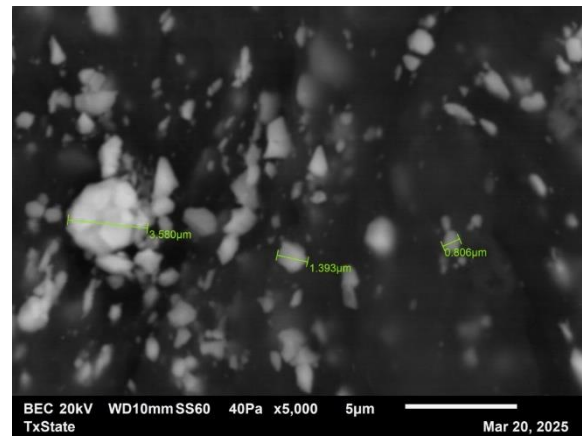


**Figure 10.** Filament with no plasticizer, 5000X

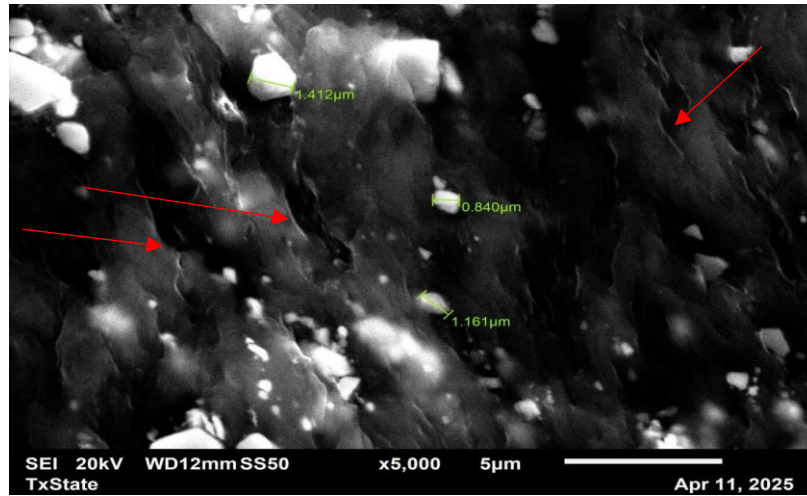


**Figure 11.** Filament with plasticizer 1000X

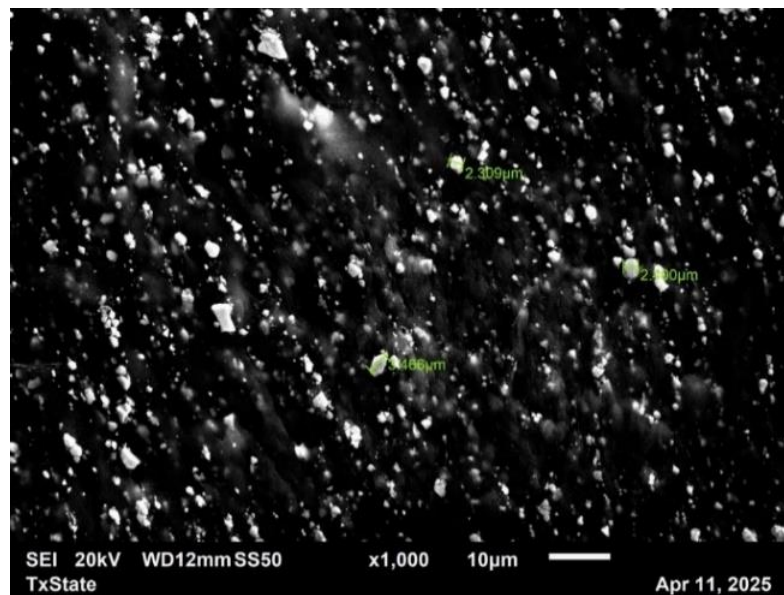


**Figure 12.** Filament with plasticizer 5000X

The main findings through the SEM are highlighted in the red arrows in Figure 11. It shows that stretching occurs in the filament. This is due to the plasticizer.

There is a method and reason for examining the samples before printing. We anticipate that some errors may occur throughout the process. It is essential to understand where these errors occur during the printing process of magnets. If the SEM images show a good filament structure compared to compromised printed parts, the assumption is that the printing process needs

adjustment. If the filament is compromised, we can halt the process to prevent wasting printing time.

SEM results of printed strontium ferrite infused PA-4,6. Shown in Figures 13 and 14 (SFO-PA4.6 composite printed).

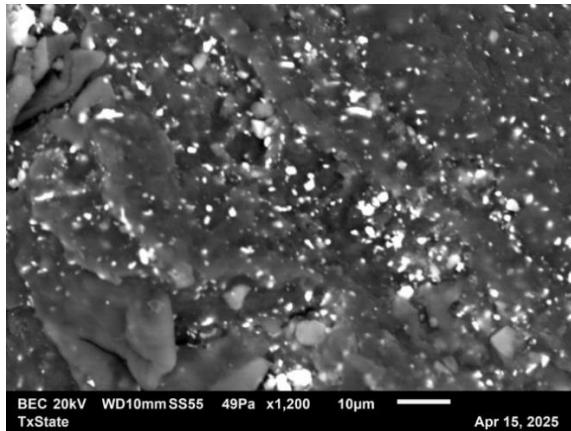


**Figure 13.** Printed part no plasticizer 1200X

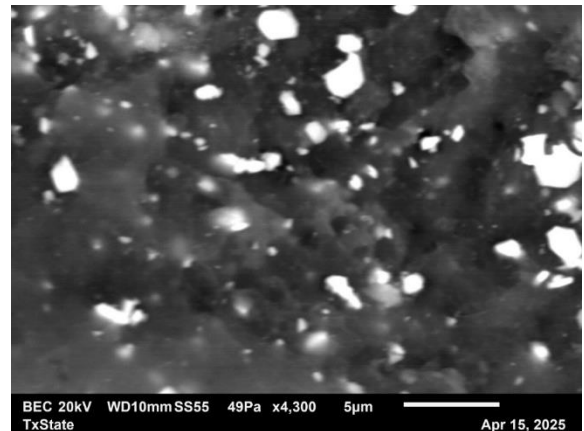


**Figure 14.** Printed part no plasticizer 4300X

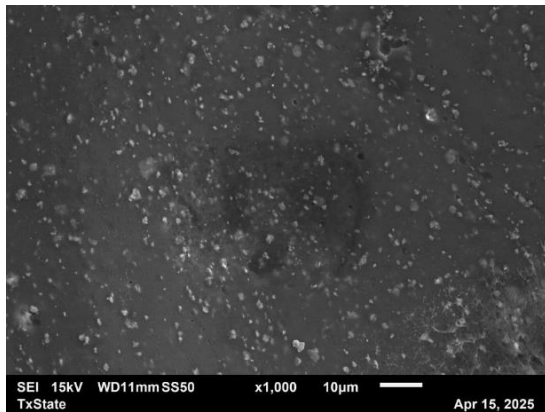


**Figure 15.** Printed part with plasticizer 1000X magnification,

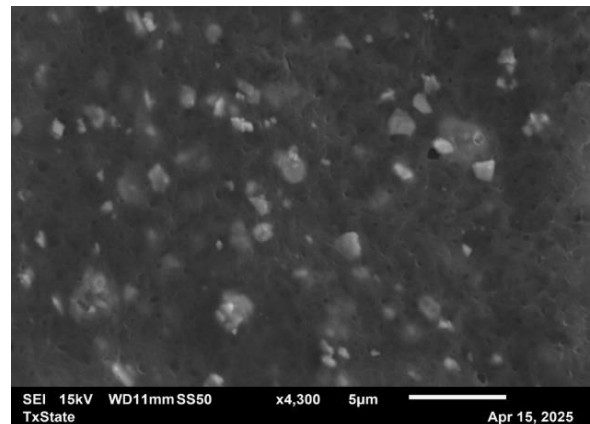


**Figure 16.** Printed part with plasticizer 4300X

Referring to the findings in the filament, we can now see that the stretching that happened along a common direction is now simply showing the porosity of the Platamid added composite mixed in the extrusion process.

One of the most significant results obtained from a Scanning Electron Microscope (SEM) is the use of energy-dispersive spectroscopy (EDS). In a JEOL SEM, the EDS system determines

the elemental composition of the sample. When the electron beam strikes the sample, it excites atoms within the material, causing them to emit characteristic X-rays. The EDS detector collects these X-rays and measures their energy, which corresponds to specific elements. By analyzing the X-ray spectrum, the system identifies and quantifies the elements present in the scanned area. This enables localized chemical analysis directly correlated with SEM imaging. The EDS data from the SEM analysis confirmed the presence of elements from PA 4,6 (C, N, and O), along with iron in the strontium ferrite.

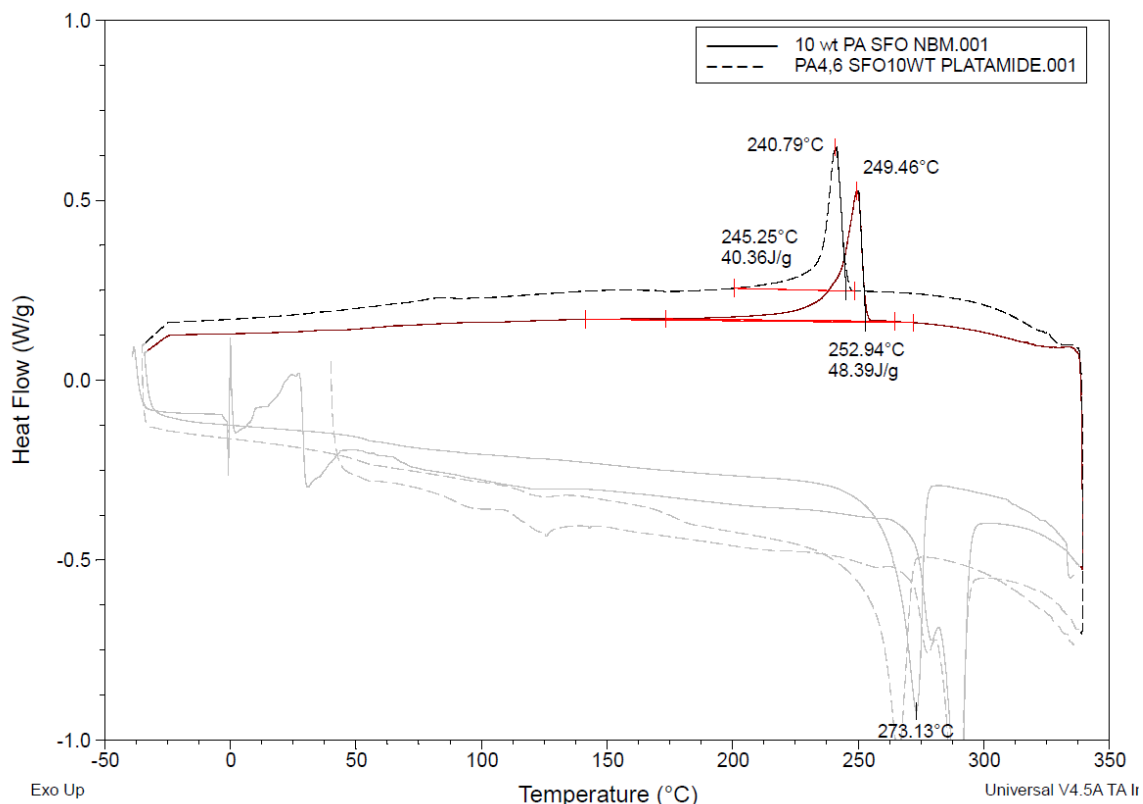


Figure 17:- DSC Heat-cool heat cycle of PA4,6-10wt% sfo and PA4,6-10wt% SFO with platamid

### 3.2 Thermal characterization

The thermal properties of the bonded magnetic composite were evaluated using Differential Scanning Calorimetry (DSC). A TA Instruments Q20 was utilized, with measurements taken from  $-40\text{ }^{\circ}\text{C}$  to  $300\text{ }^{\circ}\text{C}$ . In this characterization, printed PA 4,6 was analyzed for heat loss, moisture content, glass transition temperature (T<sub>g</sub>), and melting temperature. As shown in figure 17. The

percentage of crystallinity was then calculated and compared to the thermal analysis of PA 4,6 + 10 wt.% SFO monofilament.

Incorporating Platamid into the PA 4,6 + 10 wt.% SFO composite successfully reduced the crystallinity from 25.6% to 21.4%, representing a 16% decrease. This reduction supports the intended design objective of lowering crystallinity to enhance melt flow, interlayer diffusion, and overall printability in fused filament fabrication (FFF) processes. Platamid, a thermoplastic copolyimide adhesive, has a lower tendency to crystallize. This property likely interferes with the uniform packing and crystal growth of PA 4,6 chains, resulting in a broader and less intense melting profile. While a decrease in crystallinity is usually associated with reduced stiffness, it can also enhance ductility and improve interfacial bonding in printed composites.

### **3.3 Mechanical properties**

Bonded magnets offer a unique advantage over sintered magnets, as they are more flexible and durable, making them suitable for a wider range of applications. The evaluation of the mechanical properties of 3D-printed composites depends on the material's structural integrity, the uniform dispersion of fillers, and the efficiency of the printing process. To assess the viability of 3D printing, these properties must be compared with those of injection-molded composites. Mechanical characterization was carried out through tensile and flexural testing in accordance with ASTM D638 and ASTM D790 standards, respectively. The key parameters measured included ultimate tensile strength (UTS), elongation at break, tensile modulus, flexural strength, and flexural modulus, which serve as benchmarks for evaluating composite performance.

The mechanical performance comparison between PA4.6 Platamid + 10 wt.% SFO and PA4.6 + 10 wt.% SFO reveals clear trade-offs in strength, stiffness, and ductility. The Ultimate Tensile Strength (UTS) of the Platamid-containing composite is lower at 29.22 MPa compared to 39.93 MPa for the neat PA4.6 composite, indicating a ~27% reduction. This suggests that while Platamid may act as a processing aid or toughening agent, it compromises the load-bearing capacity of the material, possibly due to reduced interfacial bonding or plasticization of the matrix [12]. In terms of Tensile Modulus, the PA4.6 + 10 wt.% SFO composite exhibits a higher stiffness value of 3.19 GPa, compared to 2.57 GPa for the Platamid-based composite. This 24% decrease in modulus confirms that Platamid softens the matrix, resulting in lower resistance to elastic deformation.

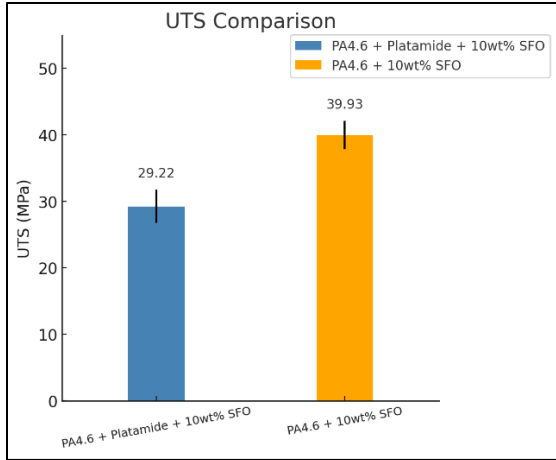


Figure 18. UTS comparison

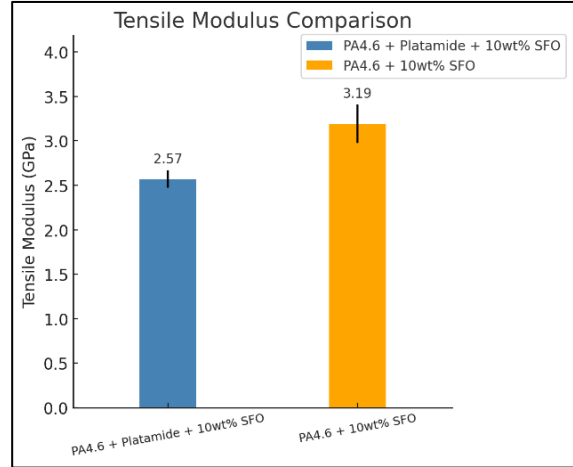


Figure 19. Tensile modulus

The comparison of mechanical performance between the composites PA4.6, Platamid + 10 wt% SFO, and PA4.6 + 10 wt% SFO highlights notable trade-offs in terms of strength, stiffness, and ductility. The Ultimate Tensile Strength (UTS) shown in Figure 18 of the composite containing Platamid is significantly lower, measured at 29.22 MPa, compared to 39.93 MPa for the neat PA4.6 composite. This represents approximately a 27% reduction in strength. This reduction suggests that while Platamid may serve as a processing aid or toughening agent, it compromises the load-bearing capacity of the material, likely due to diminished interfacial bonding or the plasticization of the matrix. Tensile Modulus Figure 19, the PA4.6 + 10 wt. The SFO composite exhibits a higher stiffness value of 3.19 GPa, whereas the Platamid-based composite has a modulus of 2.57 GPa. This indicates a 24% decrease in modulus, confirming that Platamid softens the matrix and results in lower resistance to elastic deformation.

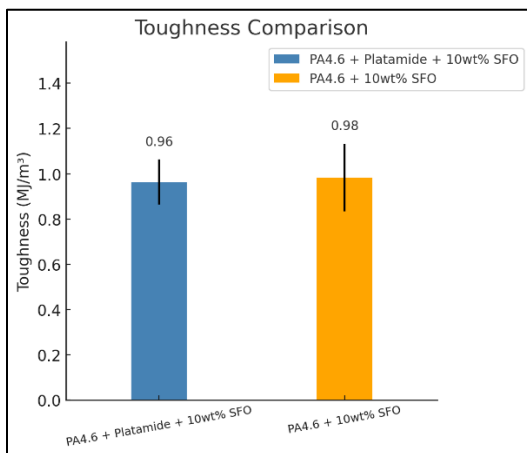


Figure 20. Equilibrium Toughness

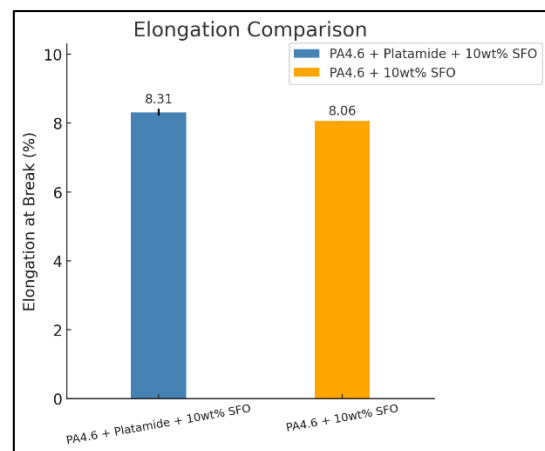


Figure 21. Elongation percentage

Interestingly, the elongation at break, shown in Figure 21, is slightly higher in the Platamid-based composite (8.31%) compared to the neat one (8.06%). This indicates improved ductility, as Platamid enhances polymer chain mobility, allowing the material to stretch further before fracture. When evaluating toughness, which represents a material's overall energy absorption capacity, both materials perform similarly. The Platamid composite exhibits a toughness of 0.96 MJ/m<sup>3</sup>, while the neat PA4.6 composite shows 0.98 MJ/m<sup>3</sup>. Although marginally lower, this suggests that the addition of Platamid does not significantly reduce the energy absorption capability of the material. Overall, incorporating Platamid into PA4.6 + SFO results in a more ductile composite but with reduced tensile strength and stiffness. This trade-off may be acceptable—or even advantageous—in applications where ease of processing is prioritized over mechanical rigidity.

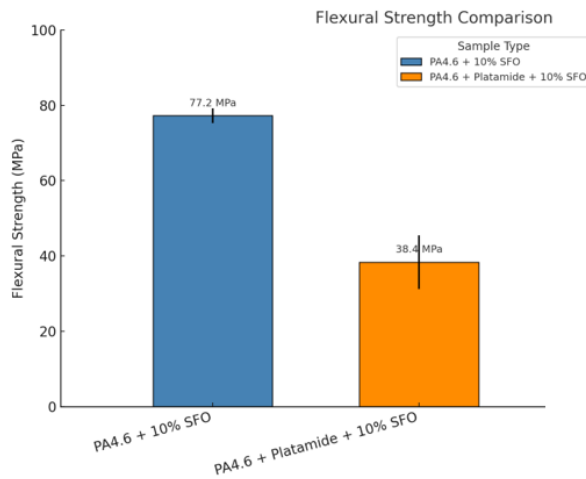


Figure 22. Flexural strength comparison

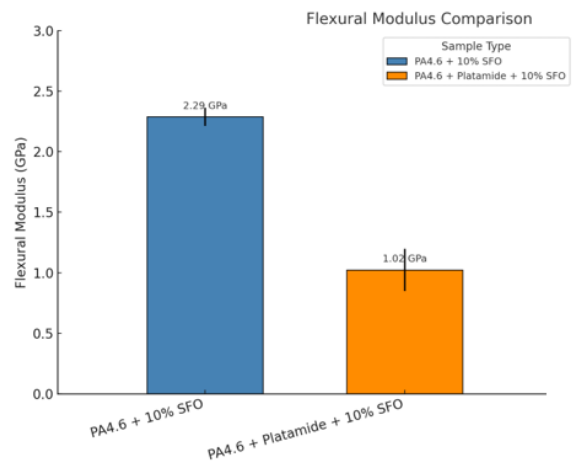


Figure 23. Flexural Modulus

Flexural tests were conducted in accordance with ASTM D790 PA 4.6, using 10wt% SFO as the reference material for comparison, as shown in Figures 22 and 23. We observed a substantial loss in flexural strength and Flexural modulus upon the addition of Platamid to the composite system. This reduction can be attributed to the decreased crystalline structure and weaker intermolecular forces between the SFO and the additive. Additionally, Platamid alters the melt viscosity of the composite, which leads to an increase in porosity in the printed composite compared to the magnetic composite alone.

## 4.0 Conclusion

This study focused on developing Polyamide 4.6-based bonded magnetic composites for functional 3D-printed magnets, addressing challenges like poor flow behavior due to high crystallinity and low melt flow index. These issues led to under-extrusion, nozzle clogging, and print defects. To improve the situation, Platamid was added to enhance melt flow and interfacial bonding. This resulted in better filament extrudability, fewer surface defects, improved inter-layer adhesion, and a more consistent deposition profile compared to control samples.

Material characterization showed uniform dispersion of  $\text{SrFe}_{12}\text{O}_{19}$  particles and robust magnetic properties after printing. Mechanical testing indicated reduced tensile strength and modulus but enhanced ductility and toughness. Thermal analysis revealed that a controlled incorporation of Platamid into the PA 4,6 + 10 wt.% SFO composite successfully reduced the crystallinity from 25.6% to 21.4% which is a 16% decrease, mitigating warping and improving thermal stability. These findings support the viability of using this composite for 3D-printed bonded magnets and contribute to research in magnetic additive manufacturing. This work lays the foundation for optimizing PA 4.6-based composites and exploring other additives or thermoplastics to enhance magnetic performance and functional applications in various fields, including medical devices and consumer electronics.

## REFERENCES

- [1] K. S. Boparai, R. Singh, and H. Singh, "Modeling and optimization of extrusion process parameters for the development of Nylon6–Al–Al<sub>2</sub>O<sub>3</sub> alternative FDM filament," *Progress in Additive Manufacturing*, vol. 1, no. 2, pp. 115–128, 2016. [Online]. Available: <https://doi.org/10.1007/s40964-016-0011-x>
- [2] Alzahrani, M., Alhumade, H., Simon, L., Yetilmezsoy, K., Madhuranthakam, C. M. R., & Elkamel, A. (2023). Additive manufacture of recycled poly (ethylene terephthalate) using pyromellitic dianhydride targeted for FDM 3D-printing applications. *Sustainability*, 15(6), 5004.
- [3] G. Chapman, A. K. Pal, M. Misra, and A. K. Mohanty, "Studies on 3D printability of novel impact modified nylon 6: Experimental investigations and performance evaluation," *Macromolecular Materials and Engineering*, vol. 305, no. 12, p. 2000548, 2020. [Online]. Available: <https://doi.org/10.1002/mame.202000548>
- [4] Department of Materials Science and Engineering, Department of Chemical Engineering, and J. U. Ogbbe, "Polymer Bonded Magnets. II. Effect of liquid crystal polymer and surface modification on Magneto-Mechanical Properties," *Polymer Composites*, vol. 21, no. 2, p. 332, 2000. [Online]. Available: <https://doi.org/10.1002/pc.10410>
- [5] C. Huber et al., "3D print of polymer bonded rare-earth magnets, and 3D magnetic field scanning with an end-user 3D printer," *Applied Physics Letters*, vol. 109, no. 16, 2016. [Online]. Available: <https://doi.org/10.1063/1.4964856>
- [6] E. M. Palmero et al., "Magnetic-polymer composites for bonding and 3D printing of permanent magnets," *IEEE Transactions on Magnetics*, vol. 55, no. 2, pp. 1–4, 2018. [Online]. Available: <https://doi.org/10.1109/tmag.2018.2863560>
- [7] J. Xiao and J. U. Otaigbe, "Polymer bonded magnets. II. Effect of liquid crystal polymer and surface modification on magneto-mechanical properties," *Polymer Composites*, vol. 21, no. 2, pp. 332–341, 2000. [Online]. Available: <https://doi.org/10.1002/pc.10197>
- [8] X. Zhang et al., "Effect of silane coupling agents on flowability and compressibility of the compound for bonded NdFeB magnet," *Journal of Rare Earths*, 2021. [Online]. Available: <https://doi.org/10.1016/j.jre.2021.05.013>

- [9] Hamat, S., Ishak, M. R., Sapuan, S. M., Yidris, N., Hussin, M. S., & Abd Manan, M. S. (2023). Influence of filament fabrication parameter on tensile strength and filament size of 3D printing PLA-3D850. *MaterialsToday:Proceedings*, 74,457-461. <https://doi.org/10.1016/j.matpr.2022.11.145>
- [10] Zhang, Y., Wang, M., Zhang, D., Wang, Y., Wang, L., Qiu, Y., ... & Zhao, L. (2023). Crystallization and performance of polyamide blends comprising polyamide 4, polyamide 6, and their copolymers. *Polymers*, 15(16), 3399.
- [11] Karkhanis, P. U., Arigbabowo, O. K., Geerts, W. J., & Tate, J. S. (2024). High-temperature 3D printing of Polyamide Magnetic Composites.
- [12] Kfoury, G., Raquez, J. M., Hassouna, F., Odent, J., Toniazzo, V., Ruch, D., & Dubois, P. (2013). Recent advances in high performance poly (lactide): from “green” plasticization to super-tough materials via (reactive) compounding. *Frontiers in chemistry*, 1, 32.